

Large cone angle magnetization precession of an individual nanomagnet with dc electrical detection

M. V. Costache, S. M. Watts, M. Sladkov, C. H. van der Wal, and B. J. van Wees
 Physics of Nanodevices, Materials Science Center, University of Groningen,
 Nijenborgh 4, 9747 AG Groningen, the Netherlands
 (dated: January 7, 2022)

We demonstrate on-chip resonant driving of large cone-angle magnetization precession of an individual nanoscale perm alloy element. Strong driving is realized by locating the element in close proximity to the shorted end of a coplanar strip waveguide, which generates a microwave magnetic field. We used a microwave frequency modulation method to accurately measure resonant changes of the dc anisotropic magnetoresistance. Precession cone angles up to 90° are determined with better than one degree of resolution. The resonance peak shape is well-described by the Landau-Lifshitz-Gilbert equation.

PACS numbers:

The microwave-frequency magnetization dynamics of nanoscale ferromagnetic elements is of critical importance to applications in spintronics. Precessional switching using ferromagnetic resonance (FMR) of magnetic memory elements¹, and the interaction between spin currents and magnetization dynamics are examples². For device applications, new methods are needed to reliably drive large angle magnetization precession and to electrically probe the precession angle in a straightforward way.

We present here strong on-chip resonant driving of the uniform magnetization precession mode of an individual nanoscale perm alloy (Py) strip. The precession cone angle is extracted via dc measurement of the anisotropic magnetoresistance (AMR), with angular resolution as low as one degree. An important conclusion from these results is that large precession cone angles (up to 90° in this study³) can be achieved and detected, which is a key ingredient for further research on so-called spin-battery effects^{4,5}. Moreover, measurements with an offset angle between the dc current and the equilibrium direction of the magnetization show dc voltage signals even in the absence of applied dc current, due to the rectification between induced ac currents in the strip and the time-dependent AMR.

Recently we have demonstrated the detection of FMR in an individual, nanoscale Py strip, located in close proximity to the shorted end of a coplanar strip waveguide (CSW), by measuring the induced microwave voltage across the strip in response to microwave power applied to the CSW⁶. However, detailed knowledge of the inductive coupling between the strip and the CSW is required for a full analysis of the FMR peak shape, and the precession cone angle could not be quantified. In other recent experiments, dc voltages have been measured in nanoscale, multilayer pillar structures that are related to the resonant precessional motion of one of the magnetic layers in the pillar^{7,8}. In one case the dc voltage is generated by rectification between the microwave current applied through the structure and its time-dependent giant magnetoresistance (GMR) effect⁸. Similar voltages

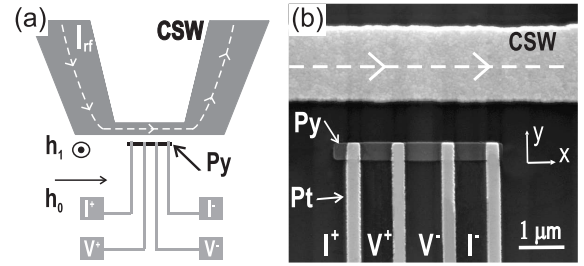


FIG. 1: (a) Schematic diagram of the device. (b) SEM picture of device with four contacts.

have been observed for a long Py strip that intersects the shorted end of a coplanar strip waveguide, which was related in part to rectification between microwave currents flowing into the Py strip and the time-dependent AMR⁹.

Fig. 1 (a) shows the device used in the present work. A Py strip is located adjacent to the shorted end of a coplanar strip waveguide (CSW) and contacted with four in-line Pt leads. The CSW, Py strip, and Pt leads were fabricated in separate steps by conventional e-beam lithography, e-beam deposition, and lift-off techniques. The CSW (and most of the contact circuit and bonding pads for the strip) consisted of 150 nm Au on 5 nm Ti adhesion layer. Fig. 1 (b) shows an SEM image of the 35 nm thick Py ($\text{Ni}_{80}\text{Fe}_{20}$) strip, with dimensions $0.3 \times 3 \mu\text{m}^2$ and the 50 nm thick Pt contacts (the Py surface was cleaned by Ar ion milling prior to Pt deposition, to insure good metallic contacts). Pt was chosen so as to avoid picking up voltages due to the "spin pumping" effect^{4,5}. An AMR response of 1.7% was determined for the strip by four-probe measurement of the difference R between the resistance when an external magnetic field is applied parallel to the current (along the long axis of the strip) and when it is applied perpendicular. This calibration of the AMR response will allow accurate determination of the precessional cone angle, as described below.

Microwave power of 9 dBm was applied from a microwave generator and coupled to the CSW (designed to have a nominal 50 Ω impedance) via electrical con-

tact with a microwave probe. This drives a microwave-frequency current of order 10 mA through the CSW, achieving the highest current density in the terminating short and thereby generating a microwave magnetic field h_1 of order 1 mT normal to the surface at the location of the strip. A dc magnetic field h_0 is applied along the long axis of the strip, perpendicular to h_1 . In this geometry we have previously shown that we can drive the uniform FM precessional mode of the Py strip⁶.

In the AMR effect, the resistance depends on the angle between the current and the direction of the magnetization as: $R(\theta) = R_0 / \cos^2 \theta$, where R_0 is the resistance of the strip when the magnetization is parallel to the direction of the current and R is the change in the resistance between parallel and perpendicular directions of the magnetization and current. When the dc current and the equilibrium magnetization direction are parallel and the magnetization of the Py undergoes circular, resonant precession about the equilibrium direction, the dc resistance will decrease by $R \sin^2 \theta_c$, where θ_c is the cone angle of the precession. Since the shape anisotropy of our Py strip causes deviation from circular precession, θ_c is an average angle of precession.

We have used a microwave frequency modulation method in order to better isolate signals due to the resonance state, removing the background resistance signal due to R_0 and dc voltage offsets in the amplifier. In this method, the frequency of the microwave field is alternated between two different values 5 GHz apart, while a dc current is applied through the outer contacts to the strip. A lock-in amplifier is referenced to the frequency of this alternation (at 17 Hz), and thus measures the difference in dc voltage across the inner contacts between the two frequencies, $V = V(f_{\text{high}}) - V(f_{\text{low}})$. Only the additional voltage given by the FMR-enhanced AMR effect will be measured when one of the microwave frequencies is in resonance.

Fig. 2(a) shows a series of voltage vs field curves in which both f_{low} and f_{high} are incremented in 1 GHz intervals, at a constant dc current of 400 A. The curves feature dips and peaks at magnetic field magnitudes corresponding to the magnetic resonant condition with either f_{high} or f_{low} , respectively. In Fig. 2(b) we focus on the peak for $f = 10.5$ GHz, and show curves for different currents ranging from -300 to +300 A. The peak height scales linearly with the current as expected for a resistive effect (Fig. 2(c)). From the slope of 1.325 mV we obtain an average cone angle $\theta_c = 4.35^\circ$ for this frequency³. Interestingly, in Fig. 2(b) a small, somewhat off-center dip is observed even for zero applied current, giving an intercept of -30 nV in Fig. 2(c). We will discuss this in detail later in the paper.

To extract information about the magnetization dynamics from the peak shape, we use the Landau-Lifschitz-Gilbert (LLG) equation, $\frac{dm}{dt} = -\gamma \mathbf{m} \times \mathbf{H} + \frac{\gamma}{m_s} \mathbf{m} \frac{dm}{dt}$, where $\mathbf{H} = (h_0 - N_x m_x; N_y m_y; h_1 - N_z m_z)$ includes the demagnetization factors N_x , N_y , and N_z (where $N_x + N_y + N_z = 1$), $\gamma = 176$ GHz/T is the gy-

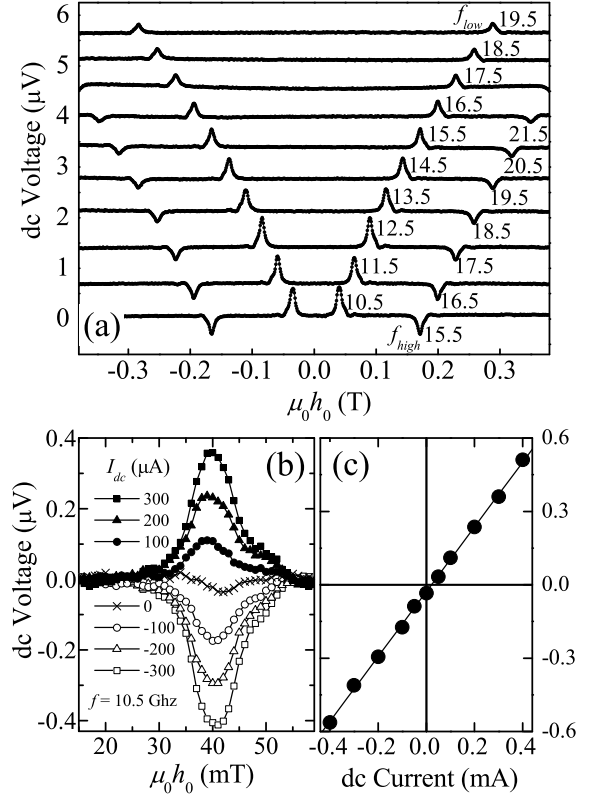


FIG. 2: (a) Dc voltage measured at $I_{dc} = 400$ A as a function of h_0 using the frequency modulation technique, where each curve represents $V = V(f_{\text{high}}) - V(f_{\text{low}})$, with $f_{\text{low}}, f_{\text{high}}$ increasing in 1 GHz increments, and $f_{\text{high}} - f_{\text{low}}$ always 5 GHz. The curves are offset for clarity. (b) The peak at $f_{\text{low}} = 10.5$ GHz for a number of currents between -300 and 300 A. (c) The peak height from the data in (b) plotted vs. the current. The line is a linear fit to the data.

romagnetic ratio, γ is the dimensionless Gilbert damping parameter and m_s is the saturation magnetization of the strip. Due to the large aspect ratio of the strip, N_x can be neglected. In the small angle limit ($\frac{dm_x}{dt} = 0$, such that $m_x \approx m_s$) the LLG equation can be linearized. In response to a driving field $h_1 \cos \omega t$ with angular frequency ω , we express the solutions as a sum of in-phase and out-of-phase susceptibility components, so $m_y = \chi_y'(\omega) h_1 \cos \omega t + \chi_y''(\omega) h_1 \sin \omega t$ and $m_z = \chi_z'(\omega) h_1 \cos \omega t + \chi_z''(\omega) h_1 \sin \omega t$. The components for m_y are as follows:

$$\chi_y'(\omega) = \frac{m_s}{2h_c + m_s} \frac{\frac{\omega}{\gamma}^2 (h_0 - h_c)^2 + \omega^2}{\omega^2} \quad (1)$$

$$\chi_y''(\omega) = \frac{m_s}{2h_c + m_s} \frac{\frac{\omega}{\gamma} (h_0 - h_c)}{\omega^2 (h_0 - h_c)^2 + \omega^2}.$$

The components of m_z are related to those of m_y by $\chi_z' = \chi_y' - \frac{\omega}{\gamma} (h_c + N_y m_s)$ and $\chi_z'' = \chi_y'' + \frac{\omega}{\gamma} (h_c + N_y m_s)$. The resonance field h_r for the uniform precessional mode is related to ω by Kittel's

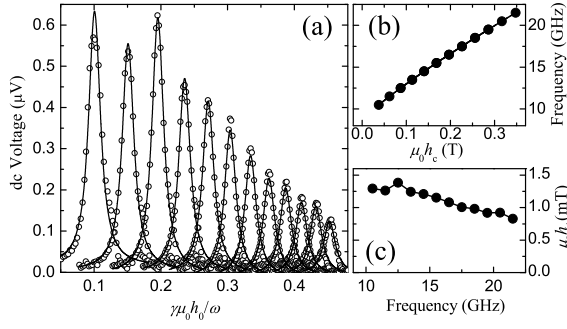


FIG. 3: (a) Resonant peaks at various frequencies ranging from 10.5 to 21.5 GHz in 1 GHz steps, as a function of the field h_0 normalized to the frequency. Solid lines are the fits of Eq. 3 to the data. (b) The frequency of the peak vs. its center position h_c . The line is a fit of Eq. 2 to the data. (c) The field h_0 calculated from the coefficients to the data in (a) and (b), as a function of frequency.

equation:

$$\dot{\phi}^2 = \frac{2}{\gamma} \frac{\partial}{\partial t} (h_c + (1 - N_y) m_s) (h_c + N_y m_s) : \quad (2)$$

The precession angle $\phi_c(t)$ is determined from the relation $\sin \phi_c(t) \dot{\phi}_c(t) = \frac{1}{m_s} (m_y^2 + m_z^2)$. We find that ϕ_c^2 can be written as the sum of a time-independent term and terms with time-dependence at twice the driving frequency, $\phi_c^2 = \phi_{dc}^2 + \phi_c^2(2!t)$, where $\phi_{dc}^2 = \frac{1}{2} \frac{h_1}{m_s} \frac{\omega_y^2}{\omega_y} + \frac{\omega_y^2}{\omega_y} + \frac{\omega_z^2}{\omega_z} + \frac{\omega_z^2}{\omega_z}$. The change in dc voltage due to the AMR effect is then $V = I_{dc} R \sin^2 \phi_{dc}$, $I_{dc} R \phi_{dc}^2$. Evaluating ϕ_{dc}^2 gives the result

$$V = A \frac{1}{\frac{1}{\gamma} \phi_{dc}^2 (h_0 - h_c)^2 + \phi_{dc}^2} ; \quad (3)$$

where $A = \frac{1}{2} I_{dc} R \frac{h_1}{2h_c + m_s} \frac{1}{1 + \frac{1}{\gamma} \phi_{dc}^2 (h_c + N_y m_s)^2}$.

Each peak from the data shown in Fig. 2(b) has been averaged with peaks at the same frequency, and replotted in Fig. 3(a) as a function of $\gamma\mu_0 h_0$. The solid lines are fits of Eq. 3 to the data, in which A and h_c are free fit parameters for each curve, and we have required to be the same for all of the peaks, resulting in a best-fit value $\gamma = 0.0104$. A plot of the frequency vs the center position of each peak h_c is shown in Fig. 3(b). The excellent fit of Eq. 2 to the data verifies that this is the uniform precessional mode, and yields values of $\mu_0 m_s = 1.06$ T and $N_y = 0.097$ as fit parameters. With these values we can extract the driving field h_1 from the peak fit parameter A (Fig. 3(c)). In agreement with our initial estimates, the field is of order 1 mT, but drops off by roughly a factor of two between 10 and 20 GHz, consistent with frequency dependent attenuation of our microwave cables and probes.

We now discuss the observation of dc voltages in the absence of any applied dc current. It has been recently

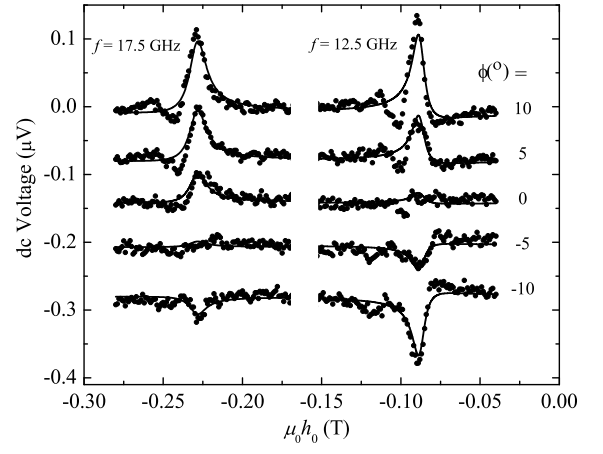


FIG. 4: Voltage peaks at $f = 17.5$ GHz (left) and at $f = 12.5$ GHz (right) without any applied current. Curves are plotted for different angles between the applied magnetic field h_0 and the long axis of the strip.

reported⁸ that when a microwave frequency current is applied through a GMR pillar structure, a dc mixing voltage is measured due to rectification between the GMR and the current. In our device, there are microwave currents induced in the strip and detection circuit due to (parasitic) capacitive and inductive coupling to the CSW structure, and thus there is the possibility for rectification between the time-dependent AMR and induced microwave currents. We express the induced current as $I_{in} = I_1 \cos !t + I_2 \sin !t$, which is true regardless of whether the induced current is caused by inductive or capacitive coupling with the CSW.

For rectification to occur, the resistance must also have first harmonic components. As mentioned earlier, the elliptical precession of the magnetization gives a time-dependent term for the cone angle $\phi_c^2(2!t)$, but this is only at the second harmonic and cannot produce rectification. However, if there is an offset angle between the applied field and the long axis of the strip, then the resistance of the ferromagnet is approximately given by

$$R(t) = R_0 + R \sin^2 \phi + \frac{m_y(t)}{m_s} \sin 2\phi ; \quad (4)$$

obtained by taking a small angle expansion of $\phi_y(t) = \frac{m_y(t)}{m_s}$ about ϕ . Multiplying with the current yields a dc voltage term

$$V_{dc} = \frac{1}{2} \frac{h_1}{m_s} R (I_1 \phi_y + I_2 \phi_y) \sin 2\phi : \quad (5)$$

Fig. 4 shows resonance peaks at $f = 17.5$ GHz and at $f = 12.5$ GHz for various different angles between the applied field and the long axis of the strip. The zero angle ($\phi = 0$) is with respect to the geometry of our device, however since we cannot see the submicron strip it is quite likely there is some offset angle ϕ_0 at this position. For the 17.5 GHz data, rotating the field by 5 causes

the peak to practically disappear. At 10 the peak reverses sign. This is in agreement with Eq. 5, with an offset angle $\phi_0 = 5^\circ$. However, the data at $f = 12.5$ GHz shows almost no peak signal already at $\phi = 0$ even though there has been no change in the setup. Moreover, in this data we more clearly see contribution from a dispersive lineshape, corresponding to the $I_2^{(0)}$ term in Eq. 5. For each frequency, we fit Eq. 5 to all the curves simultaneously, where we have used the parameters for the magnetization extracted earlier and allowed only I_1 , I_2 and an offset angle ϕ_0 to be free parameters. For the 17.5 GHz data, we obtain $\phi_0 = 6.1^\circ$, $I_1 = 28$ A, and $I_2 = 8$ A. For the 12.5 GHz data, we obtain $\phi_0 = 1.5^\circ$, $I_1 = 23$ A, and $I_2 = 11$ A. At both frequencies, the induced current is mostly in phase with the driving frequency, and roughly one-tenth to one-hundredth of the current flowing through the CSW short. The large difference in ϕ_0 between 12.5 GHz and 17.5 GHz is likely due to a frequency dependence of the induced currents and how they flow through the Pt contacts to the Py. Such a contact effect is also a likely explanation for some features in the data, such as small peaks and dips occurring to the left (higher field magnitude) of the primary peaks

in Fig. 4, that are not easily described by our model. Similar features can also be observed in Fig. 2(a).

As concluding remarks, we note that the range of applicability of our technique is broader than has been presented here. For the purposes of this experiment we have used a relatively long strip geometry with four in-line contacts. However, two contacts are sufficient and there is no particular limit to how small the ferromagnetic element can be, as long as it can be electrically contacted and dc current applied along the equilibrium magnetization direction. In terms of resolution, we estimate that precessional cone angles as low as one degree can readily be resolved. As for the other extreme, in the data presented here we have used only modest applied microwave power. In other experiments we have driven much larger precession angles with upwards of 20 dBm of power. We finally note that the rectification effect may be used to detect when the element is in resonance and can give information about induced microwave currents in the structure even when a dc current is not applied.

This work was financially supported by Fundamenteel Onderzoek der Materie (FOM). We acknowledge J. Jungmann for her assistance in this project.

¹ S. Kaka and S. E. Russek, Appl. Phys. Lett. 80, 2958 (2002).

² M. Tsoi, A. G. M. Jansen, J. Bass, W.-C. Chiang, V. Tsoi and P. Wyder, Nature 406, 46 (2000).

³ At 13 dBm of applied power, we have measured an angle of $\phi_c = 9.0^\circ$ at $f = 10.5$ GHz. We focus here on the 9 dBm data however, since we can apply this power over the entire 10 to 25 GHz bandwidth.

⁴ A. Brataas, Y. Tserkovnyak, G. E. W. Bauer, and B. I. Halperin, Phys. Rev. B 66, 060404(R) (2002).

⁵ M. V. Costache, M. Sladkov, S. M. Watts, C. H. van der Wal, and B. J. van Wees, cond-mat/0609089.

⁶ M. V. Costache, M. Sladkov, C. H. van der Wal, and B. J. van Wees, to be published in Appl. Phys. Lett.; cond-mat/0607036.

⁷ A. A. Tulapurkar, Y. Suzuki, A. Fukushima, H. Kubota, H. Muehara, K. Tsunekawa, D. D. D. Jayaprawira, N. Watanabe, and S. Yuasa, Nature 438, 339 (2005).

⁸ J. C. Sankey, P. M. Baganca, A. G. F. Garcia, I. N. Krievorotov, R. A. Buhrman, and D. C. Ralph, Phys. Rev. Lett. 96, 227601 (2006).

⁹ A. Yamaguchi, T. Ono, Y. Suzuki, S. Yuasa, A. Tulapurkar, and Y. Nakatani, cond-mat/0606305.